2006

Identification of source locations in two-dimensional heat equations

Leevan Ling
Hong Kong Baptist University, lling@hkbu.edu.hk

Masahiro Yamamoto

Y. C. Hon

Tomoya Takeuchi

Citation
Ling, Leevan, Masahiro Yamamoto, Y. C. Hon, and Tomoya Takeuchi. "Identification of source locations in two-dimensional heat equations." *Inverse Problems* 22.4 (2006): 1289-1305.

Identification of source locations in two-dimensional heat equations

Leevan Ling

Department of Mathematics, Hong Kong Baptist University, Hong Kong.

E-mail: lling@hkbu.edu.hk

Masahiro Yamamoto

Graduate School of Mathematical Sciences, University of Tokyo, Japan.

E-mail: myama@ms.u-tokyo.ac.jp

Y. C. Hon

Department of Mathematics, City University of Hong Kong, Hong Kong.

E-mail: maychon@cityu.edu.hk

Tomoya Takeuchi

Graduate School of Mathematical Sciences, University of Tokyo, Japan.

E-mail: take@ms.u-tokyo.ac.jp

Abstract. In this paper, we give the uniqueness on the identification of unknown source locations in two-dimensional heat equations from scattered measurements. Based on the assumption that the unknown source function is a sum of some known functions, we prove that one measurement point is sufficient to identify the number of sources and three measurement points are sufficient to determine all unknown source locations. For verification, we propose a numerical reconstruction scheme for recovering the number of unknown sources and all source locations.

3 May 2006

1. Introduction

Inverse source identification problems are important in many branches of engineering sciences. For example, an accurate estimation of pollutant source [7] is crucial to environmental safeguard in cities with high population. In general, a complete recovery of the unknown source is not attainable from practically restricted boundary measurements. The inverse source problem becomes solvable if certain *a priori* knowledge is assumed. Inverse problems are in nature *unstable* because the unknown solutions/ parameters have to be determined from indirect observable data which contain measurement errors. The major difficulty in establishing any numerical algorithm for approximating the solution is the severe ill-posedness of the problem and the ill-conditioning of the resultant discretized matrix.

The heat conduction process is irreducible in time, while the temperature profile becomes rapidly smoother in time. This means that the characteristic of the solution may not be affected by the observed data. To the knowledge of the authors, the mathematical analysis and efficient algorithms for inverse heat problems are still very limited. For instance, the uniqueness and conditional stability results for heat source identification problem can be found in [3, 5, 17]. Studies on stationary point source problem can be found in [2, 6, 11]. Some reconstruction schemes can be found in [15, 16, 19, 20].

Consider a heat equation of the form

$$\partial_t \widetilde{u}(x,\, t) = \triangle \widetilde{u}(x,\, t) + h(t) f(x), \qquad x = (x_1,\, x_2) \in \mathbb{R}^2,\; t > 0, \tag{1}$$

with initial condition

$$\widetilde{u}(x, 0) = 0, \qquad x \in \mathbb{R}^2. \tag{2}$$

In this paper we give a sufficient condition to determine the unknown source function $f(x)$, which is assumed to be a spatially density function of the sources, from some scattered measurements. We also assume that the function $h(t)$ in equation (1) can be modelled as a known time dependent function. In other words, the source function f in (1) is of a special form and is assumed to be the sum of a known function $\rho \in \mathscr{S}(\mathbb{R}^2)$,

$$f(x) = \sum_{k=1}^{N} \rho(x - a_k) \in \mathscr{S}(\mathbb{R}^2), \tag{3}$$

where $a_1, \ldots, a_N$ are mutually distinct and $\mathscr{S}$ is the space of rapidly decreasing functions. The methodology in this paper also works under the assumption that $\rho \in L^1(\mathbb{R}^2)$. The function ρ is either radially symmetric or a product of two even functions $\widetilde{\rho}$ in $\mathbb{R}$, namely $\rho(x) = \widetilde{\rho}(x)\widetilde{\rho}(y)$. Moreover, we assume that

$$\int_{\mathbb{R}^2} \rho(z)\, dz > 0.$$

This form of $f(x)$ models heat sources which concentrate near a_k, $1 \le k \le N$ with the same unit strength. For example, in the case where the heat is provided by a single kind of radioactive isotope, we can set $h(t) = e^{-\lambda t}$ with a constant $\lambda > 0$. In particular,

the form f can simulate point sources at a_k given by the Dirac delta function $\delta(x-a_k)$, which can be justified if the respective supports of the sources near a_k are sufficiently small. Thus one can consider that the determination of f of form (3) is practical if we can assume that all the sources near a_k have the unit strength.

Equivalently, we will discuss an inverse problem of the form

$$\begin{cases} \partial_t u(x,t) = \Delta u(x,t) + f(x), & x=(x_1,x_2)\in\mathbb{R}^2,\ t>0, \\ u(x,0)=0, & x\in\mathbb{R}^2. \end{cases} \tag{4}$$

If we set $v(x,t)=\partial_t u(x,t)$, then

$$\partial_t v(x,t) = \Delta v(x,t), \qquad x\in\mathbb{R}^2,\ t>0, \tag{5}$$

and from equations (2) and (4) we have

$$v(x,0) = f(x), \qquad x\in\mathbb{R}^2. \tag{6}$$

Suppose $h\in C^1[0,\infty)$ and $h(0)\neq 0$. If v satisfies (5) and (6), then we can directly verify that

$$\widetilde{u}(x,t) \equiv \int_0^t h(t-s)\, v(x,s)ds, \quad x\in\mathbb{R}^2,\ t>0,$$

satisfies (1) and (2). Notice that

$$\widetilde{u}(x,t) \equiv \int_0^t h(s)\, v(x,t-s)ds, \quad x\in\mathbb{R}^2,\ t>0.$$

Differentiating both sides of the above equation with respect to t, we have

$$\partial_t\widetilde{u}(x,t) = h(0)\, v(x,t) + \int_0^t h'(t-s)\, v(x,s)ds, \quad x\in\mathbb{R}^2,\ t>0.$$

Since $h(0)\neq 0$, this is a *Volterra equation* of the second kind. For any given observation data at x_0, we can stably recover $v(x_0,t)$ from $\partial_t\tilde{u}(x_0,t)$ by using some iterative methods. The above inverse problem (1) with $h(t)$ is then reduced to the inverse problem stated in (4) if we choose $\widetilde{u}(b_j,t)$, $1\le j\le M$, $0\le t\le t_1$, as observation data where $M\in\mathbb{N}$ and $t_1>0$ are fixed. It is noted here that for more general parabolic equations, our proposed method can be extended by using approximate fundamental solutions through kernels generating functions. In this paper, we focus only on the two-dimensional heat equation given in the form of (4).

The *Inverse source identification problem* is now stated as follows:

> Determine a number N and N unknown source locations $\{a_k\}_{1\le k\le N}\subset\mathbb{R}^2$ in (4) by some observation data
>
> $$u(b_j,t), \quad 1\le j\le M,$$
>
> where $M\in\mathbb{N}$ and $t\in(t_0,t_1)$ with $0<t_0<t_1$ are fixed.

The organization of this paper is as follow. The main theorem on the uniqueness in our inverse problem is firstly presented in Section 2. Followed by some proofs on lemmas and related theorems in Section 3, the proof of the main theorem 7 is given in Section 4.

For numerical verification, on the basis of theorem 7, a novel computational scheme is proposed in Section 5 to identify the unknown source locations based on the theoretical result that only three measurement points are sufficient. Finally, the conclusion is given in Section 6.

2. Main theorem

Denote $v(x,t) = \partial_t u(x,t)$. The solution $v(x,\, t)$ of (5)–(6) is then given by

$$\begin{aligned} v(x,t) &= \frac{1}{4\pi t}\int_{\mathbb{R}^2} \exp\left(-\frac{|x-z|^2}{4t}\right) f(z)\, dz \\ &= \sum_{k=1}^{N} \frac{1}{4\pi t}\int_{\mathbb{R}^2} \exp\left(-\frac{|x-z|^2}{4t}\right) \rho(z-a_k)\, dz, \end{aligned}$$

and hence the solution for (4) is given by

$$\begin{aligned} u(x,\, t) &= \int_0^t v(x,\, \tau)\, d\tau \\ &= \sum_{k=1}^{N} \int_0^t \int_{\mathbb{R}^2} \frac{1}{4\pi\tau} \exp\left(-\frac{|x-z|^2}{4\tau}\right) \rho(z-a_k)\, dz\, d\tau. \end{aligned} \tag{7}$$

Since the source locations are unknown, the solution $u(x,t)$ of equation (7) can be approximated by the method of fundamental solutions [1, 4, 8, 9]:

$$u_n(x,t) = \sum_{i=1}^{P} \lambda_{u,i} \int_0^t \int_{\mathbb{R}^2} \frac{1}{4\pi\tau} \exp\left(-\frac{|x-z|^2}{4\tau}\right) \rho(z-\xi_i)\, dz\, d\tau, \tag{8}$$

where $\lambda_{u,i} \in \mathbb{R}$, $\{\xi_i\}_{i=1}^{P} \subset \mathbb{R}^2$, $P \in \mathbb{N}$ is a set of distinct trial centers. Here, P can be infinity for the sake of analysis. Moreover, the approximate source function $f_n(x)$ corresponding to the approximation u_n is given as

$$f_n(x) = f_n(x; \lambda_{u,i}) \equiv \partial_t u_n(x,\, 0) = \sum_{i=1}^{P} \lambda_{u,i}\, \rho(x-\xi_i), \tag{9}$$

which lies in the space $\mathscr{S}(\mathbb{R}^2)$. The unknown coefficients $\lambda_{u,i}$ in (8) are obtained by solving a collocation system with data taken at some given measurement points with discrete time sampling rate.

For the well-posed direct problem where the source function f is known, since the numerical approximation $u_n(x,t)$ given in (8) satisfies sufficient collocation condition, it can be expected that the numerical solution reasonably approximates the exact solution. In the case of inverse problems, the ill-posed and non-uniqueness nature induce extreme difficulties in handling, for instance, the inverse source identification posed in this paper.

The imposed collocation condition implies that $u_n(b_j, t) = u(b_j, t)$ for all $j = 1, \ldots, M$ and $t \in (t_0, t_1)$. We define the *difference* by $w = u_n - u$ and obtain from equations (7) and (8) that

$$\begin{aligned} w(x,\, t) &\equiv u_n(x,\, t) - u(x,\, t) \\ &= \sum_{i=1}^{P+N} \lambda_{w,i} \int_0^t \int_{\mathbb{R}^2} \frac{1}{4\pi\tau} \exp\left(-\frac{|x-z|^2}{4\tau}\right) \rho(x-\xi_i)\, dz\, d\tau, \end{aligned} \tag{10}$$

where $a_k = \xi_{P+k}$ and $\lambda_{w,P+k} = -1$ for all $k = 1, \ldots, N$. The difference function w automatically satisfies the initial condition:

$$w(b_j,\, t) = 0, \quad j = 1, \ldots, M, \quad \text{for all } t \in (t_0,\, t_1),$$

and the heat equation

$$\partial_t w(x,\, t) = \triangle w(x,\, t) + g(x), \qquad x \in \mathbb{R}^2,\ t > 0, \tag{11}$$

where $g \in \mathscr{S}(\mathbb{R}^2)$ is the source function corresponding to the difference function w as

$$g(x) \equiv [f_n - f](x) = \sum_{i=1}^{P+N} \lambda_{w,i}\, \rho(x-\xi_i) \in \mathscr{S}(\mathbb{R}^2). \tag{12}$$

Here, f is the unknown source function in (4) and f_n is the source corresponding to the approximation u_n defined in (9). Throughout the paper, we study the properties of the coefficients $\lambda_{w,i}$ appeared in the difference function w in (10) and the source function g in (12).

If we can conclude that $g = 0$ identically, then the inverse source identification problem has a unique solution. Unfortunately, this is not the case for $M = 1$. The main theorem of this paper stated in the following is to show that $M = 3$ measurement points are sufficient to determine N and all source locations in (3):

Theorem 1 *Let $b_1,\ b_2,\ b_3 \in \mathbb{R}^2$ be measurement points that are not colinear. The data at these three points*

$$u(b_1, t),\ u(b_2, t),\ u(b_3, t), \quad \textit{for all } t \in (t_0,\, t_1),$$

uniquely determines all source locations $a_1, \ldots, a_N \in \mathbb{R}^2$ of the unknown source function (3) *in the heat equation* (4).

Some lemmas and related theorems will be proved in the following section before giving the proof of the main theorem in Section 4.

3. Case with one measurement

We consider only one point measurement $u(b_1, t)$ where $b_1 \in \mathbb{R}^2$ is fixed. In this section, we prove the *power sum* equality based on the unknown coefficients in (12).

Let u_n^* be a numerical approximation with finite terms P that agrees with the exact solution $u(b, t_\ell) = u_n^*(b, t_\ell)$ at a finite sequence of distinct collocation points such that $t_\ell \in (t_0,\ t_1)$ for all $\ell = 1, \ldots, Q$. We define a subspace $\mathcal{K}(b_1, \ldots, b_M)$ by

$$\overline{\text{Span}\ \left\{\exp\left(-\eta^2|z-b_i|^2\right):\ 1 \le i \le M,\ \eta^2 = \frac{1}{4t},\ \forall t \in (0, t_0)\right\}}, \tag{13}$$

which is the closure of the space spanned by all Gaussian functions centering at b_j, $j = 1, \ldots, M$ with different shape parameters η. The closure in (13) is taken in the space $L^2(\mathbb{R}^2)$.

Lemma 2 *If $\varphi(x) := \phi(|x|^2)$ for some $\phi \in L^2(\mathbb{R}^+)$, then $\varphi \in \mathcal{K}(0)$.*

Proof. Let

$$X = \left\{\varphi \in L^2(\mathbb{R}^2):\ \varphi(x) = \phi(|x|^2) \text{ for some } \phi(x) \in L^2(\mathbb{R}^+)\right\}.$$

Since $\varphi_n \to \varphi$ in $L^2(\mathbb{R}^2)$ implies $\varphi_n \to \varphi$ almost everywhere in $\mathbb{R}^2$ and the convergence keeps the form of φ in X, we see that X is closed in $L^2(\mathbb{R}^2)$ and hence is a Hilbert space with L^2-scalar product. In order to complete the proof, it is sufficient to prove that $\varphi \in X$ and

$$\int_{\mathbb{R}^2} \varphi(x) \exp\left(-\eta^2|x|^2\right) dx = 0, \quad \eta > \frac{1}{4t_0},$$

imply $\varphi(x) = 0$, $x \in \mathbb{R}^2$. Setting $r = \sqrt{x_1^2 + x_2^2}$, we introduce the polar coordinate:

$$\begin{aligned}\int_{\mathbb{R}^2} \varphi(x) \exp\left(-\eta^2|x|^2\right) dx &= 2\pi \int_0^\infty \varphi(r^2) \exp\left(-\eta^2 r^2\right) r\, dr \\ &= \pi \int_0^\infty \varphi(p) \exp\left(-\eta^2 p\right)\, dp = 0,\end{aligned}$$

with $\eta^2 > 1/(16t_0^2)$. This means that the Laplace transform of $\varphi(p)$ vanishes on a segment. By using the analyticity of the Laplace transform and the unicity theorem of the analytic function, we know that the Laplace transform of φ vanishes identically. Hence $\varphi = 0$ in $\mathbb{R}^2$. □

Henceforth we set $B(b_1; R) = \{x \in \mathbb{R}^2 : |x - b_1| < R\}$.

Corollary 3 *The subspace $K(b_1)$ defined in* (13) *contains the characteristic function $\chi_{B(b_1;R)}$ for any $R > 0$.*

Proof. This corollary follows immediately from Lemma 2 with a shift from the origin to b_1 and by picking $\tilde{\varphi} = H(0) - H(R)$ where H is the Heaviside function in $\mathbb{R}$. □

The following theorem implies that the numerical solution u_n obtained from using this collocation method is not unique. Moreover, the numerical solution u_n will not approximate the desired exact solution u no matter how large one takes the values of P and M.

Theorem 4 *Let $w(x,\, t)$ be a solution of* (11) *with $g \in \mathscr{S}(\mathbb{R}^2)$. Furthermore, we assume that the solution $w(x,\, t)$ is identically zero along $w(b_1,\, t)$ for some $b_1 \in \mathbb{R}^2$ and for all $t \in (t_0,\, t_1)$. Then the source function g in* (11) *must satisfy*

$$\int_{\mathbb{R}^2} g(z)\, dz = 0, \quad \textit{and} \quad N = \sum_{i=1}^{P} \lambda_{u,i}.$$

Proof. Without loss of generality, we assume $b_1 = 0$ for simplicity. The condition $w(0,\, t) = 0$ for $t \in (t_0,\, t_1)$ implies

$$\partial_t w(0,\, t) = \frac{1}{4\pi t} \int_{\mathbb{R}^2} \exp\left(-\frac{|z|^2}{4t}\right) g(z)\, dz = 0, \quad \text{for all } t \in (t_0,\, t_1).$$

Therefore, the following condition is also true:

$$\int_{\mathbb{R}^2} \exp\left(-\frac{|z|^2}{4t}\right) g(z)\, dz = 0, \quad \text{for all } t \in (t_0,\, t_1). \tag{14}$$

Since the left-hand side of (14) is analytic, we can complete the proof by using analytic extension and a limiting process with $t \to \infty$ (using the Lebesgue convergence theorem [10]). For illustration, we will complete the proof without using analytic extension.

¿From (14), the source function $g \in \mathscr{S}(\mathbb{R}^2)$ satisfies

$$\int_{\mathbb{R}^2} K(z)\, g(z)\, dz = 0, \quad \text{for all } K \in \mathcal{K}(b_1). \tag{15}$$

For any $\epsilon > 0$, there exists a $R > 0$ such that if we pick $K = \chi_{B(0;R)}$, then

$$\begin{aligned}
\left|\int_{\mathbb{R}^2} g(z)\, dz\right| &\le \underbrace{\left|\int_{\mathbb{R}^2} \chi_{B(0;R)} g(z)\, dz\right|}_{=0} + \left|\int_{\mathbb{R}^2} (1 - \chi_{B(0;R)}) g(z)\, dz\right| \\
&\le \underbrace{\left|\int_{B(0;R)} (1 - \chi_{B(0;R)}) g(z)\, dz\right|}_{=0} \\
&\qquad + \left|\int_{\mathbb{R}^2 \setminus B(0;R)} (1 - \chi_{B(0;R)}) g(z)\, dz\right| \\
&< \epsilon.
\end{aligned}$$

The second equality follows directly from (12). □

Theorem 4 highlights the fact that collecting data at only one measurement point is sufficient only to determine the total number of sources (i.e., the net force). From the numerical point of view, we have

$$\int_{\mathbb{R}^2} g(z)\, dz = \epsilon_{P,M},$$

for some $\epsilon_{P,M} \to 0$ as $P,\ M \to \infty$. Furthermore, from (3) and (9), we have an approximation to the *net force*

$$\sum_{i=1}^{P} \lambda_{u,i} = N + C_\rho\, \epsilon_{P,M},$$

where $C_\rho\, \epsilon_{P,M} = \left(\int_{\mathbb{R}^2} \rho(z)\, dz\right)^{-1} \epsilon_{P,M}$ is the *net force approximation error*.

Lemma 5 *Under the same assumptions stated in Theorem 4, the expansion coefficients* $\lambda_{w,i}$ *of the difference function* w *in* (10) *must satisfy*

$$\sum_{i=1}^{P+N} |b_1 - \xi_i|^2 \, \lambda_{w,i} = 0 \in \mathbb{R}^2.$$

Proof. By the similar argument given in the proof of Theorem 4 and using Lemma 2, we can pick $K(z) = \chi_{B(b_1;R)}|z - b_1|^2$ for a sufficiently large R depending on ϵ. Then, we have

$$\begin{aligned}
0 &= \int_{\mathbb{R}^2} |z - b_1|^2 \, g(z) \, dz \\
&= \int_{\mathbb{R}^2} \sum_{i=1}^{P+N} \lambda_{w,i} \, |z - b_1|^2 \, \rho(z - \xi_i) \, dz \\
&= \int_{\mathbb{R}^2} \sum_{i=1}^{P+N} \lambda_{w,i} \, |z - (b_1 - \xi_i)|^2 \, \rho(z) \, dz \\
&= \int_{\mathbb{R}^2} \sum_{i=1}^{P+N} \lambda_{w,i} \left(|z|^2 - 2(b_1 - \xi_i)^T z + |b_1 - \xi_i|^2 \right) \rho(z) \, dz \\
&= \int_{\mathbb{R}^2} |z|^2 \, \rho(z) \, dz \left(\sum_{i=1}^{P+N} \lambda_{w,i} \right) - 2 \sum_{i=1}^{P+N} \lambda_{w,i} (b_1 - \xi_i)^T \left(\int_{\mathbb{R}^2} z \, \rho(z) \, dz \right) \\
&\quad + \left(\sum_{i=1}^{P+N} |b_1 - \xi_i|^2 \, \lambda_{w,i} \right) \int_{\mathbb{R}^2} \rho(z) \, dz.
\end{aligned}$$

The first two terms of the above equation vanish due to the fact that $\sum_{i=1}^{P+N} \lambda_{w,i} = 0$ using Theorem 4 and $\int_{\mathbb{R}^2} z \, \rho(z) \, dz = 0$ by the assumption. Since $\int_{\mathbb{R}^2} \rho(z) \, dz$ is non-zero, we must have

$$\sum_{i=1}^{P+N} |b_1 - \xi_i|^2 \, \lambda_{w,i} = 0,$$

and the lemma is proven. □

Theorem 6 *Under the same assumptions stated in Theorem 4, the expansion coefficients* $\lambda_{w,i}$ *of the difference function* w *in* (10) *must satisfy*

$$\sum_{i=1}^{P+N} |b_1 - \xi_i|^{2p} \, \lambda_{w,i} = 0 \in \mathbb{R}^2, \quad p \in \mathbb{N}.$$

Proof. Based on the fact that $\chi_{B(b_1;R)}|x - b_1|^{2p} \in \mathcal{K}(b_1)$ for all $R > 0$ and $p \in \mathbb{N}$, this theorem follows inductively from Lemma 5. □

We now give the proof of the main Theorem 1 in the following section.

4. Source identification by three measurements

Denote $r_{j,k} \equiv |b_j - a_k|$. From Theorem 6, we construct for each $j = 1, 2, 3$ the power sum

$$\sum_{k=1}^{N} (r_{j,k})^{2p} = \left(\sum_{i=1}^{P} |b_j - \xi_i|^{2p} \lambda_{u,i} \right), \quad p \in \mathbb{N}. \tag{16}$$

The right-hand side of (16) can be approximated by the numerical solution u_n^*. For each measurement point b_j, the nonlinear system (16) is related to the *elementary symmetric polynomials*. Using the *Newton-Girard formulas* [12], the system of N equations given by (16) with $p = 1, \ldots, N$ is equivalent to

$$\left\{ \begin{array}{rcl} r_{j,1}^2 + r_{j,2}^2 + r_{j,3}^2 + \ldots + r_{j,N}^2 &=& -\alpha_1, \\ r_{j,1}^2 \cdot r_{j,2}^2 + r_{j,1}^2 \cdot r_{j,3}^2 + \ldots + r_{j,N-1}^2 \cdot r_{j,N}^2 &=& +\alpha_2, \\ & \vdots & \\ r_{j,1}^2 \cdot r_{j,2}^2 \cdots r_{j,N}^2 &=& (-1)^N \alpha_N, \end{array} \right. \tag{17}$$

for some $\alpha_1, \ldots, \alpha_N$ depending only on ξ_i and $\lambda_{u,i}$. Consider a polynomial of degree N with respect to z of the form

$$f(z) = z^N + \alpha_1 z^{N-1} + \ldots + \alpha_N.$$

From (17), we can easily see that $f(r_{j,k}^2) = 0$ for all $k = 1, \ldots, N$. This yields

$$f(z) = (z - r_{j,1}^2) \cdot (z - r_{j,2}^2) \cdots (z - r_{j,N}^2).$$

Hence, we can determine all $r_{j,k}$ as the roots of the polynomial f.

It is well known that any three circles in the $\mathbb{R}^2$-plane with distinct centers which are not colinear have at most one common intersection point. Consequently $\{r_{1,k}, r_{2,k}, r_{3,k}\}$ can determine a unique source point a_k if b_1, b_2, b_3 are not colinear. Proof of Theorem 1 is hence completed.

It is noted here that the sufficient condition $M = 3$ given in Theorem 1 on the source identification problem is not minimal. For $M = 2$, we have two sets of circles centering at b_1 and b_2 that can provide a finite number of candidates for the source location a_k. Moreover, equation (15) could provide extra information on top of Theorem 6. For example, if $\rho(x) = \exp(-\varepsilon^2 |x|^2)$ is also a Gaussian, by picking

$$K(z) = \exp\left(-\gamma(t)^2 |b_j - z|^2\right) \in \mathcal{K}(b_j),$$

for $j = 1, 2$ and we can obtain another nonlinear systems

$$\sum_{j=1}^{P+N} \frac{\pi \lambda_{w,j}}{\gamma(t)^2 + \varepsilon^2} \exp\left(\frac{-\gamma(t)^2 \varepsilon^2 {r_{j,k}}^2}{\gamma(t)^2 + \varepsilon^2} \right) = 0, \quad \text{for all } \gamma(t) = \frac{1}{4t},\ t \in (t_0, t_1).$$

This extra information can be used to identify the right candidate from the finite set obtained by $M = 2$ measurement points. We do not study in this paper the minimum number of the observation points for the problem but for practical application, it is more interesting to study the case of multiple measurement points. The above discussion

suggests also that our observations $u(b_j, t)$, $1 \le j \le M$ can uniquely determine also the strengths $\gamma_k \neq 0$, $\gamma_k \in \mathbb{R}$, $1 \le k \le N$ if we replace (3) by

$$f(x) = \sum_{k=1}^{N} \gamma_k \rho(x - a_k)$$

but we will not here discuss further.

Theorem 7 *With data from three non-colinear measurement points, the expansion coefficients $\lambda_{w,i}$ of w in* (10) *must satisfy*

$$\sum_{i=1}^{P+N} (\xi_i - \zeta)\ \lambda_{w,i} = 0 \in \mathbb{R}^2,$$

and

$$\sum_{i=1}^{P+N} |\xi_i - \zeta|^2\, \lambda_{w,i} = 0 \in \mathbb{R},$$

for all $\zeta \in \mathbb{R}^2$.

Proof. From Theorem 6, for $1 \le j \le M = 3$ we have

$$\begin{aligned} 0 &= \sum_{i=1}^{P+N} |b_j - \xi_i|^2\, \lambda_{w,i} \\ &= \sum_{i=1}^{P+N} \left(|b_j|^2 - 2b_j^T \xi_i + |\xi_i|^2\right)\ \lambda_{w,i} \\ &= \sum_{i=1}^{P+N} \left(-2b_j^T \xi_i + |\xi_i|^2\right)\ \lambda_{w,i}. \end{aligned} \tag{18}$$

The last equality follows from Theorem 4. Subtracting consecutive equations in (18) results in

$$\begin{aligned} (b_1 - b_2)^T \sum_{i=1}^{P+N} \xi_i\, \lambda_{w,i} = 0, \\ (b_1 - b_3)^T \sum_{i=1}^{P+N} \xi_i\, \lambda_{w,i} = 0. \end{aligned}$$

If $M = 3$ and the measurement points $b_j = (b_{j,1},\ b_{j,2})^T$, $j = 1, 2, 3$ are non-colinear, then the following matrix

$$\begin{bmatrix} b_{1,1} - b_{2,1} & b_{1,2} - b_{2,2} \\ b_{1,1} - b_{3,1} & b_{1,2} - b_{3,2} \end{bmatrix}$$

is nonsingular and hence both elements in $\sum_{i=1}^{P+N} \xi_i \lambda_{w,i}$ must vanish. Using Theorem 4, we obtain $\sum_{i=1}^{P+N} \zeta \lambda_{w,i} = 0$ for all $\zeta \in \mathbb{R}$. The first assertion is proven. Moreover,

$$\sum_{i=1}^{P+N} |\xi_i|^2 \lambda_{w,i} = 0,$$

follows immediately from (18) and the first assertion. Hence, the second assertion is also true. □

Theorem 7 provides the first and second moment equations about the unknown source locations. The first moment equations (for $\zeta = b_j$) can be used to reduce the complexity of the nonlinear problems in Theorem 1. If more than three measurement points are available, we can obtain higher moment equations by induction.

5. Numerical Verifications

In this section, we will verify the numerical efficiency of the different factors contained in the equalities proven in the last section. Since the reconstruction procedure is based on the proven uniqueness results *using one set of measurement data*, the provided data should be redundant in order to overcome the presence of noise, i.e., $M > 3$ measurement points or $M = 3$ with repeated measurements. If the data is noisy, some standard regularization technique (e.g. Tikhonov regularization with the L-curve method) should be applied to the linear system solver and the proposed method can still provide reasonable accuracy to the estimations of the measurement-to-source distance. We leave the study of noisy data to our future research. Here we focus on the noise free case.

Without loss of generality, assume the set of source locations $\{a_k\}_{1\le k\le N}$ and the set of measurement points $\{b_j\}_{1\le j\le M}$ are both contained in an open domain $\Omega \subset \mathbb{R}^2$. At first, the function $\rho(x)$ in (3) is $\exp(-|x|^2)$. All (discrete) data are obtained by either a single measurement point b_1 or all three measurement points given by

$$\begin{aligned} b_1 &= (0,\, 1),\\ b_2 &= (1/\sqrt{2},\, -1/\sqrt{2}),\\ b_3 &= (-1/\sqrt{2},\, -1/\sqrt{2}), \end{aligned}$$

at some sampling times t_ℓ for $1 \le \ell \le Q$ such that $t_\ell \in [10^{-10}, T_{\max}]$ is equally distributed. The trial centers ξ_i are uniformly placed within the unit circle Ω; whereas the source locations a_k are randomly placed in Ω unless otherwise specified. A demonstration is given in Figure 1. In our computations, the linear systems are solved by using Matlab's MLDIVID and the nonlinear systems for locating $r_{j,k}$ are solved by the Levenberg-Marquardt method [13, 14].

In order to verify the numerical efficiency of Theorem 4, we investigate the effect of increasing numbers of trial centers P for the cases when only *one measurement point* b_1 is used. The range for the sample time $T_{\max}$ is set to be 20. Three sets of $N = 1$, 10, and 20 source points are tested. As P increases from 1 to 20, approximation errors of all cases show a linear trend in the LOG-Y plot as shown in Figure 2 which implies exponential convergence. The value of P is tested up to 100 to show that the numerical computation is stable. Although some oscillations are observed, the approximation of the total number of sources N is rather stable with respect to the number of trial points. Furthermore, the accuracy is independent of the number of source points N.

Figure 3 studies the effect of increasing the numbers of sampling times Q with various values of $T_{\max} = 1$, 5, 20, and 100. The number of trial centers is fixed at $P = 40$. Similarly to Figure 2, we also observe a monotone trend as Q increases from a small value up to 10. The value $T_{\max}$ has a direct influence to the discretized sets of $\mathcal{K}(b_1)$ in (13); larger values of $T_{\max}$ result in more distinct basis and therefore show better accuracy.

Moreover, we verify the first equality given in Theorem 7 by using all three measurement points and $\zeta = 0$. In Figure 4, the numerical error of the first moment $\sum_{i=1}^{P+N} \xi_{i,1}\, \lambda_{w,i}$ is displayed. In this computation the number of sampling times is $Q = 40$ for $T_{\max} = 100$ and the numbers of source points are $N = 1$, 10, and 20 respectively. It can be observed from Figure 4 that the accuracy is independent of the number of source points. The error profiles of the other first moment $\sum_{i=1}^{P+N} \xi_{i,2}\, \lambda_{w,i}$ and the second equality in Theorem 7 behave similarly and are omitted here.

Next, the unknown measurement-to-source distances required in the proof of Theorem 1 are identified from three measurement points. Here, the number of trial points is $P = 50$ and the number of sampling times is $Q = 100$ between $[10^{-10}, 100]$. Three different cases are studied:

Case 1: All sources are widely spread within Ω. Tested source points $\{a_k\}_{k=1}^{N}$ are:

Example 1: $\{(.4, 0), (-.26, .13), (-.36, -.33)\}$,
Example 2: $\{(.4, 0), (-.26, .13), (-.36, -.33), (.25, .65)\}$,
Example 3: $\{(.4, 0), (-.26, .13), (-.36, -.33), (.25, .65), (.2, -.65)\}$.

Case 2: Some sources are clustered within Ω.

Example 4: $\{(.4, 0), (.401, 0), (-.36, -.33)\}$,
Example 5: $\{(.4, 0), (.401, 0), (-.36, -.33), (-.36, -.34)\}$.

Case 3: Some sources lie outside of the artificial domain $\overline{\Omega}$.

Example 6: $\{(.4, 0), (-.26, .13), (1, 1)\}$,
Example 7: $\{(.4, 0), (-.26, .13), (1, 1), (-1, -1)\}$.

The last Case 3 refers to the situation when some source points are not surrounded by the trial centers. This is an numerical test case corresponding to an incorrect selection of the artificial domain and is independent of our previous definition of Ω in Section 2. Once all the measurement-to-source distances $r_{j,k}$ are computed by using equation (16),

Example	$\{b_1, b_2, b_3\}$	$\{b'_1, b'_2, b'_3\}$
1	4.6853e-6	*0*
2	*3.9968e-4*	4.7113e-4
3	*2.0071e-2*	2.1012e-2
4	4.9536e-4	*4.1372e-4*
5	7.6023e-3	*4.6668e-3*
6	1.1119e-3	*7.1978e-5*
7	*5.6113e-2*	8.7644e-2

Table 1. Maximum error in the approximated distances $r_{j,k}$ using two sets of measurement points.

the source locations are identified by computing the intersection of the three circles, see Figure 5 for illustration. There are two possibilities for the presence of numerical errors. First, the $r_{j,k}$ are overestimated. This results in a small region of intersection which will be regarded as numerical error. On the other hand, if the $r_{j,k}$ are underestimated, there will have no intersection. In our computations, we progressively increase all $r_{j,k}$ until some nonempty regions are found. An algorithm for finding such intersections of circles was proposed by Vakulenko [18]. Successful numerical identification of source locations strongly depends on the geometry of the unknown source locations and the measurement points. In the following, only the error in $r_{j,k}$ will be reported. To refine the estimation on the source locations with *a priori* estimation, other numerical method can be applied, for instance see [11].

The accuracies in finding $r_{j,k}$ for the three Case 1 to Case 3 are displayed in Figure 6 to Figure 8 respectively. The order of $r_{j,k}$ are sorted according to its error in absolute value. All plots are displayed in the same scale for easy comparison. In general, the numerical efficiency of Theorem 7 drops as the value of P increases. Furthermore, due to the complexity of the nonlinear systems, the accuracy is better in the case of smaller N. For Example 1, all errors lie between 3.2E-7 to 4.7E-6. On the other hand, with $N = 5$ source points in Example 3, the errors lie between 6.6E-5 and 2.0E-2. The maximum errors for Example 5 and Example 7 are 7.6E-3 and 5.6E-2, respectively. Numerical performance on all these cases appears to be similar.

Finally, instead of using equally distributed measurement points, we allocate the measurement points more close to the upper part of the domain. Namely,

$$b'_1 = (0,\, 1),$$
$$b'_2 = (1/\sqrt{2},\, 1/\sqrt{2}),$$
$$b'_3 = (-1/\sqrt{2},\, 1/\sqrt{2}).$$

Figure 9 demonstrates the errors in approximating the distances for Examples 2, 4 and 7. The maximum errors in both sets of measurement points are summarized in Table 1. In general, both sets of measurement points result in similar accuracy (except for Examples 1 and 6 in which the $\{b'_1, b'_2, b'_3\}$ set results in much smaller error).

6. Conclusion

In this paper, we study the source identification problem for two-dimensional heat equations. The source function is assumed to be the sum of a shifted known function. Our work focuses on giving sufficient data for the uniqueness in the inverse problem. We prove that the observation data taken at three measurement points are sufficient to uniquely determine all unknown source locations. Some numerical examples are given to demonstrate the possibility of numerical reconstruction. The result of this work provides a theoretical foundation for developing practical numerical schemes for more general inverse heat source problems with noises. In such cases, more measurement points should be taken and will be a focus of our future work.

Acknowledgement

The first named author was supported partially by Grant 94-2119-M-110-015 from the National Science Council, Taiwan.
The work of the second named author was supported partially by Grant 15340027 from the Japan Society for the Promotion of Science and Grant 15340015 from the Ministry of Education, Cultures, Sports and Technology.
The third named author described in this paper was fully supported by a grant from the Research Grants Council of the Hong Kong Special Administrative Region, China (Project No. CityU 101205).
The forth named author was supported partially by the 21 century COE program at Graduate School of Mathematical Sciences, the University of Tokyo.

References

[1] C. J. S. Alves, C. S. Chen, and B. Săler. The method of fundamental solutions for solving Poisson problems. In *Boundary elements, XXIV (Sintra, 2002)*, volume 13 of *Int. Ser. Adv. Bound. Elem.*, pages 67–76. WIT Press, Southampton, 2002.

[2] L. Baratchart, A. Ben Abda, F. Ben Hassen, and J. Leblond. Recovery of pointwise sources or small inclusions in 2D domains and rational approximation. *Inverse Problems*, 21(1):51–74, 2005.

[3] J. R. Cannon and Salvador Pérez Esteva. Uniqueness and stability of 3D heat sources. *Inverse Problems*, 7(1):57–62, 1991.

[4] C. Y. Chan and C. S. Chen. Method of fundamental solutions for multi-dimensional quenching problems. In *Proceedings of Dynamic Systems and Applications, Vol. 2 (Atlanta, GA, 1995)*, pages 115–121, Atlanta, GA, 1996. Dynamic.

[5] M. Choulli and M. Yamamoto. Conditional stability in determining a heat source. *J. Inverse Ill-Posed Probl.*, 12(3):233–243, 2004.

[6] A. El Badia and T. Ha Duong. Some remarks on the problem of source identification from boundary measurements. *Inverse Problems*, 14(4):883–891, 1998.

[7] A. El Badia and T. Ha-Duong. On an inverse source problem for the heat equation. Application to a pollution detection problem. *J. Inverse Ill-Posed Probl.*, 10(6):585–599, 2002.

[8] M. A. Golberg. The method of fundamental solutions for Poisson's equation. *Eng. Anal. Boundary Elements*, 16(3):205–213, October 1995.

[9] M. A. Golberg and C. S. Chen. The method of fundamental solutions for potential, Helmholtz and diffusion problems. In *Boundary integral methods: numerical and mathematical aspects*, volume 1 of *Comput. Eng.*, pages 103–176. WIT Press/Comput. Mech. Publ., Boston, MA, 1999.

[10] Elliott H. Lieb and Michael Loss. *Analysis*, volume 14 of *Graduate Studies in Mathematics*. American Mathematical Society, Providence, RI, second edition, 2001.

[11] Leevan Ling, Y. C. Hon, and M. Yamamoto. Inverse source identification for Poisson equation. *Inverse Probl. Sci. Eng.*, 13(4):433–447, 2005.

[12] D. E. Littlewood. *A university algebra*. Dover Publications Inc., New York, 1970. An introduction to classic and modern algebra, Republication of the second (1958) edition.

[13] Donald W. Marquardt. An algorithm for least-squares estimation of nonlinear parameters. *J. Soc. Indust. Appl. Math.*, 11:431–441, 1963.

[14] Jorge J. Moré. The Levenberg-Marquardt algorithm: implementation and theory. In *Numerical analysis (Proc. 7th Biennial Conf., Univ. Dundee, Dundee, 1977)*, pages 105–116. Lecture Notes in Math., Vol. 630. Springer, Berlin, 1978.

[15] H. M. Park and J. S. Chung. A sequential method of solving inverse natural convection problems. *Inverse Problems*, 18(3):529–546, 2002.

[16] A. G. Ramm. An inverse problem for the heat equation. II. *Appl. Anal.*, 81(4):929–937, 2002.

[17] Saburou Saitoh, Vu Kim Tuan, and Masahiro Yamamoto. Reverse convolution inequalities and applications to inverse heat source problems. *JIPAM. J. Inequal. Pure Appl. Math.*, 3(5):Article 80, 11 pp. (electronic), 2002.

[18] Alexander Vakulenko. "circles intersection". Technical report, 2004. From *MATLAB Central File Exchange*–File Id: 5313. `http://www.mathworks.com/`.

[19] Ping Wang and Kewang Zheng. Reconstruction of heat sources in heat conduction equations. *Comput. Appl. Math.*, 19(2):231–238, 2000.

[20] Zh. Yi and D. A. Murio. Source term identification in 1-D IHCP. *Comput. Math. Appl.*, 47(12):1921–1933, 2004.

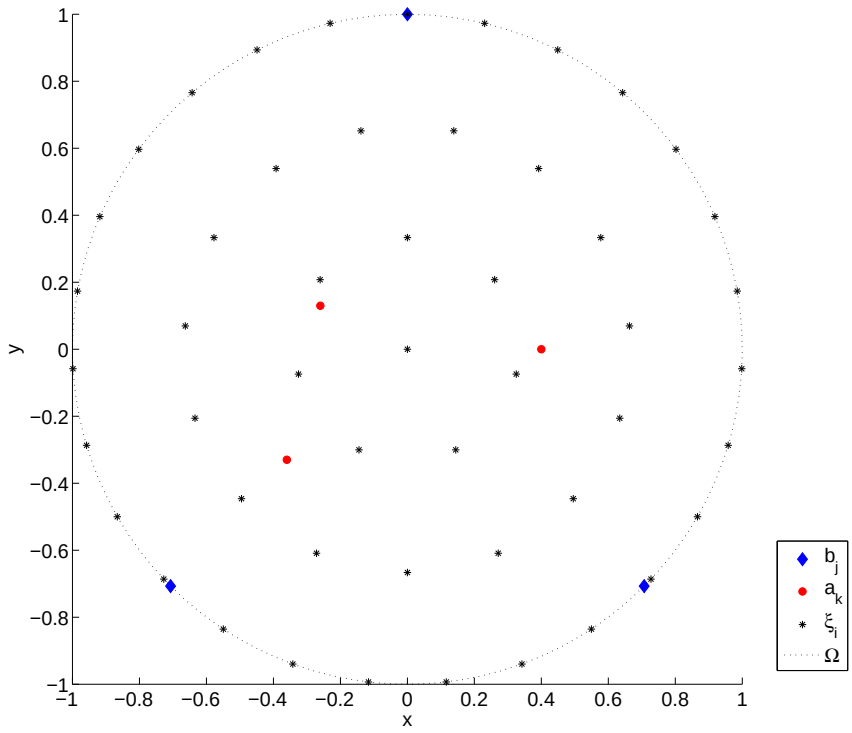

Figure 1. Sample arrangement of $M = 3$ measurement points b_j, $N = 3$ source points a_k, and $P = 50$ trial points ξ_i.

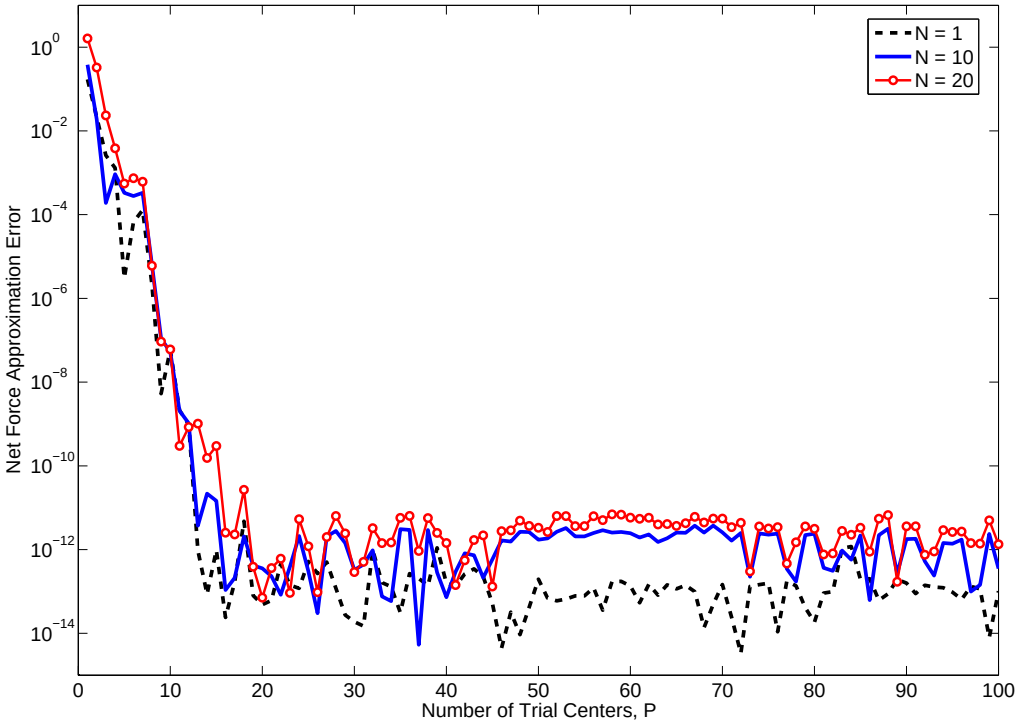

Figure 2. Approximation error to the total number of sources as a function of the number of trial centers using one measurement point. As of the title of Y-axis : error in number of sources

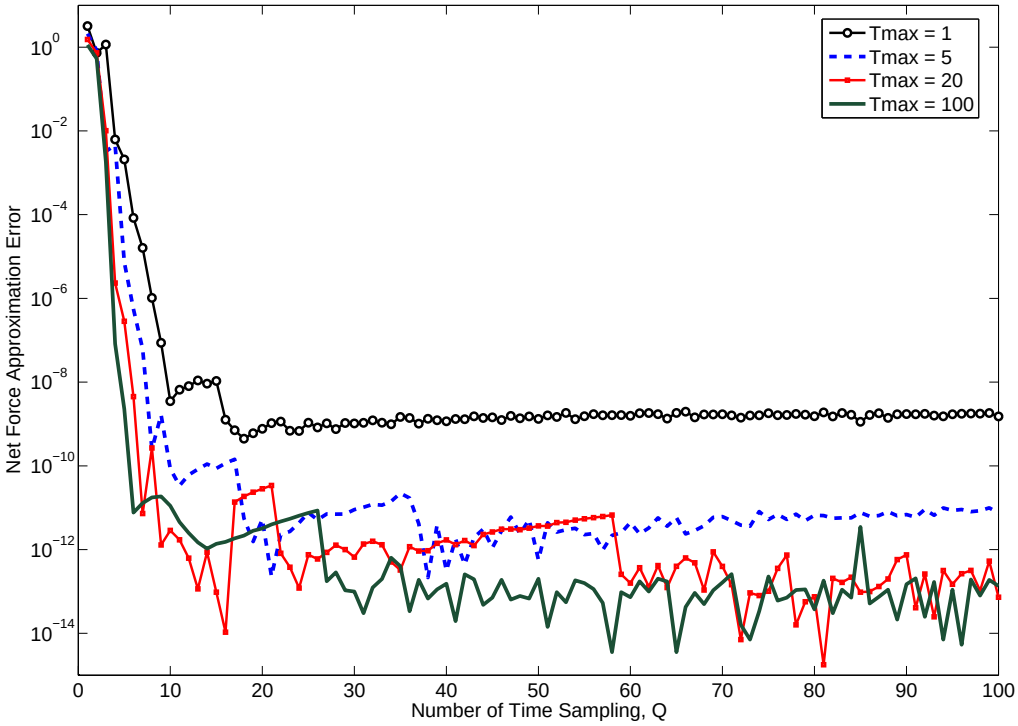

Figure 3. Approximation error to the total number of sources as a function of the number sampling times using one measurement point.

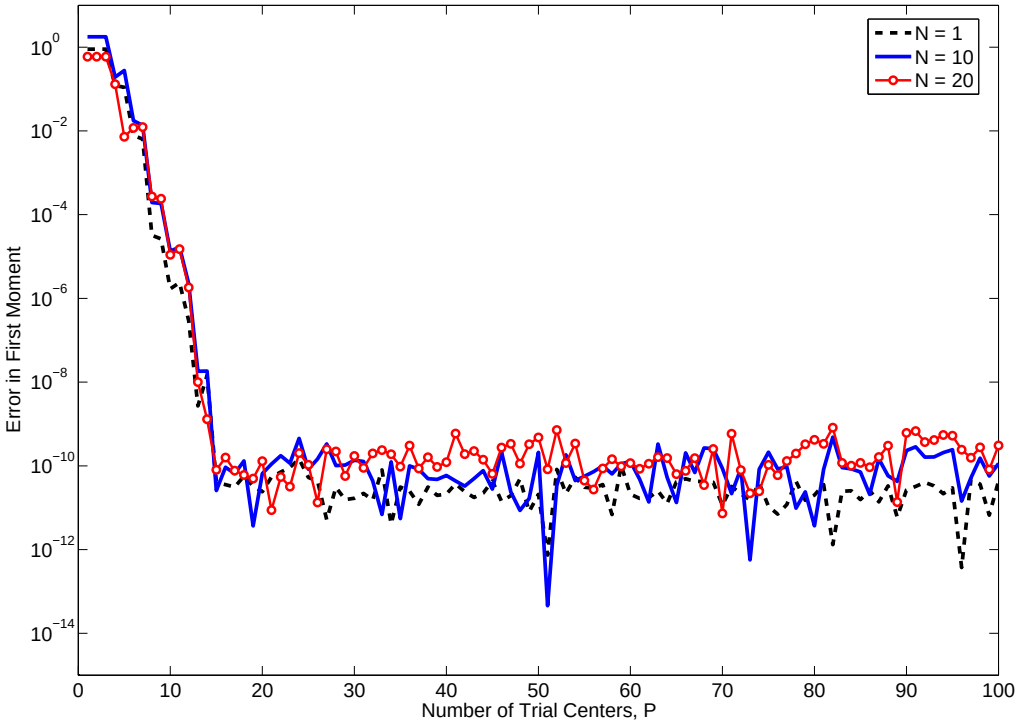

Figure 4. Error in the first moment as a function of the number of trial centers using three measurement points.

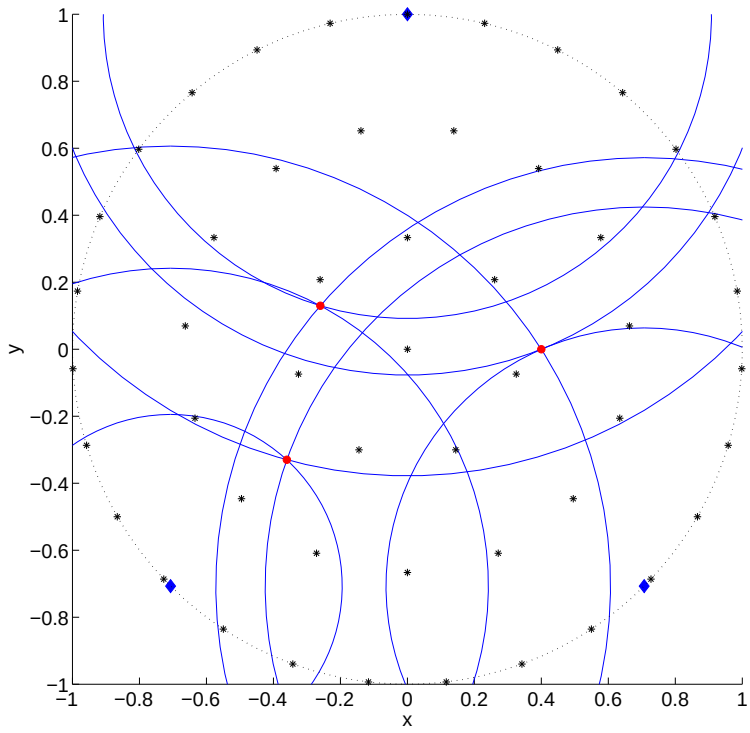

Figure 5. Finding source locations by the intersection of three circles.

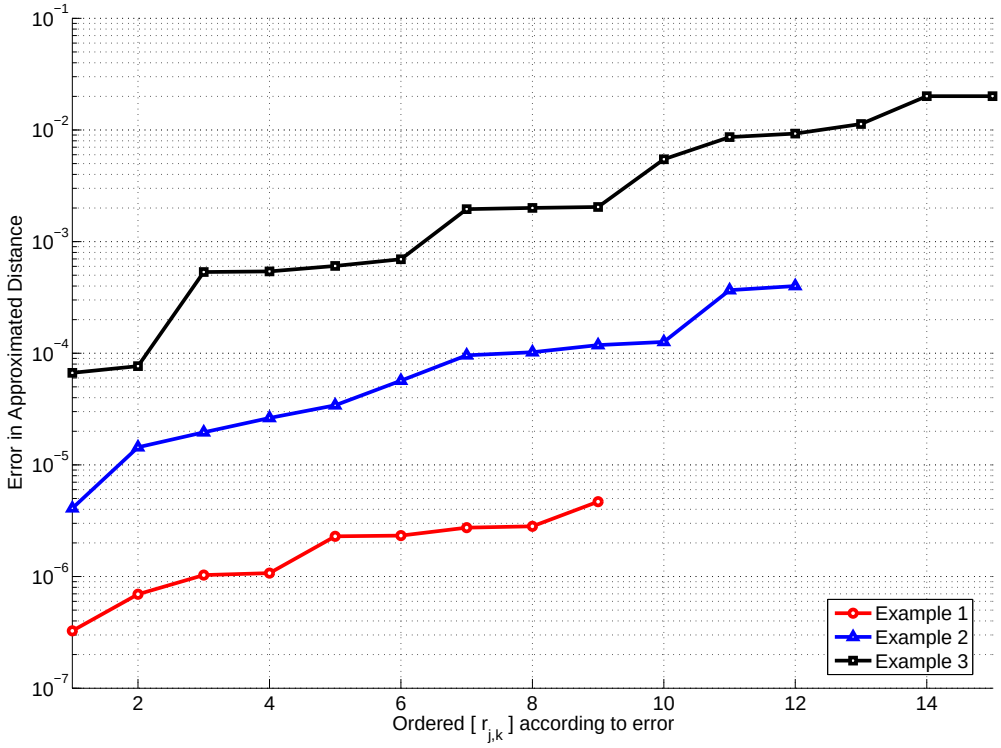

Figure 6. Case 1: Example 1 to Example 3. Error in approximate distance for each $r_{j,k}$ (sorted based on the errors), $1 \leq j \leq 3$ and $1 \leq k \leq N$ using $M = 3$ measurement points $\{b_1, b_2, b_3\}$.

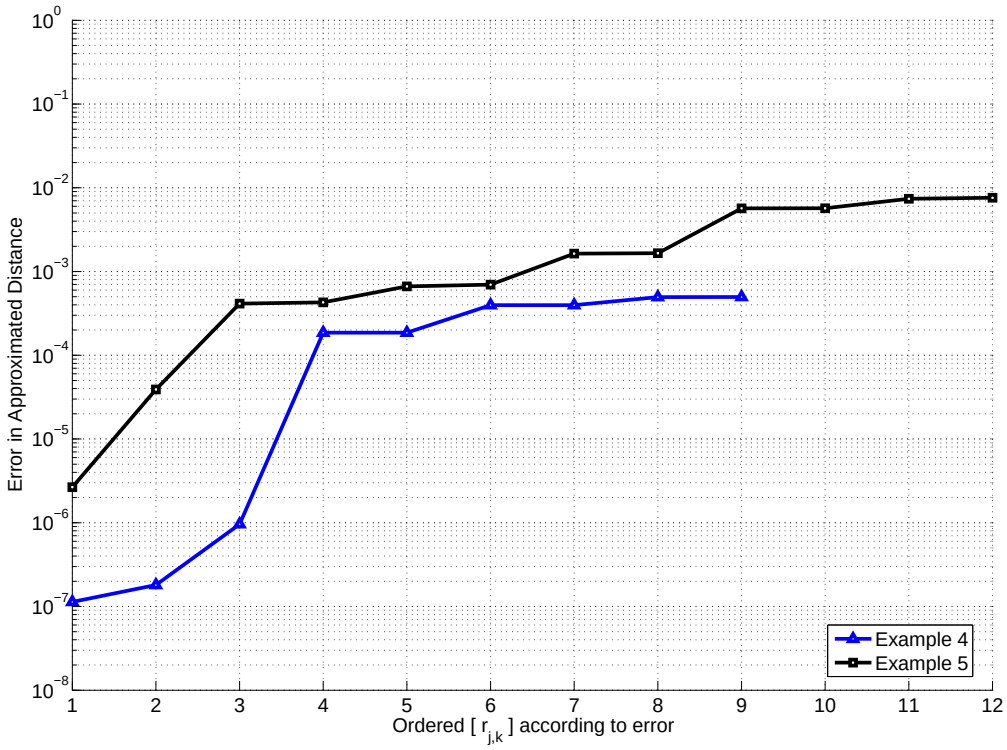

Figure 7. Case 2: Example 4 to Example 5. Error in approximate distance for each $r_{j,k}$ (sorted based on the errors), $1 \leq j \leq 3$ and $1 \leq k \leq N$ using $M = 3$ measurement points $\{b_1, b_2, b_3\}$.

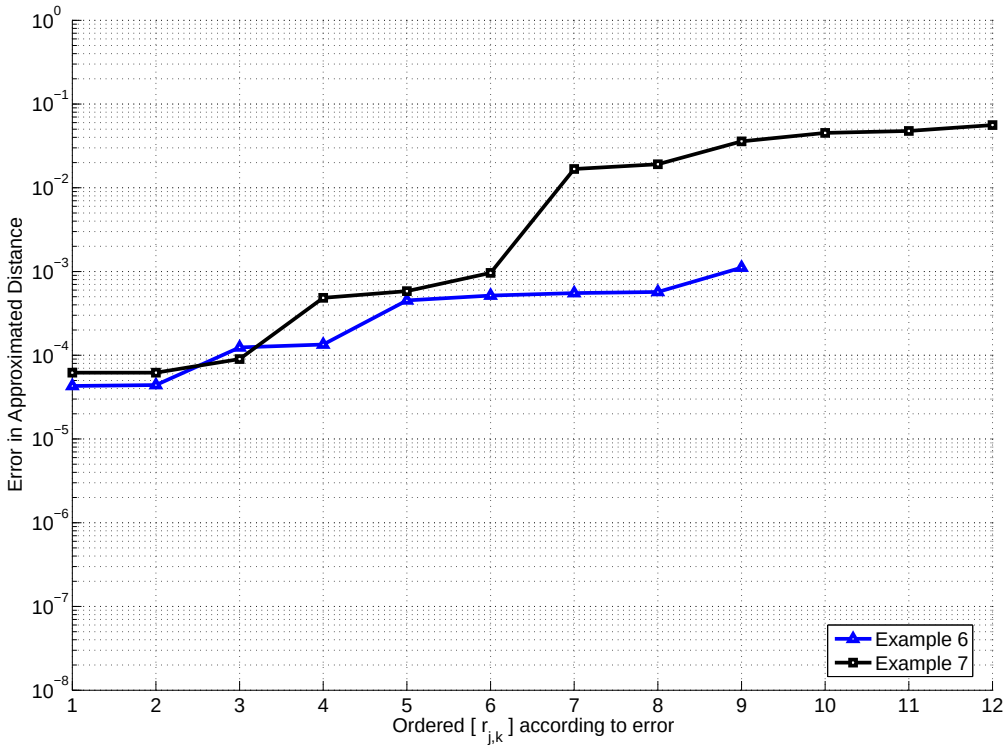

Figure 8. Case 3: Example 6 to Example 7. Error in approximate distance for each $r_{j,k}$ (sorted based on the errors), $1 \leq j \leq 3$ and $1 \leq k \leq N$ using $M = 3$ measurement points $\{b_1, b_2, b_3\}$.

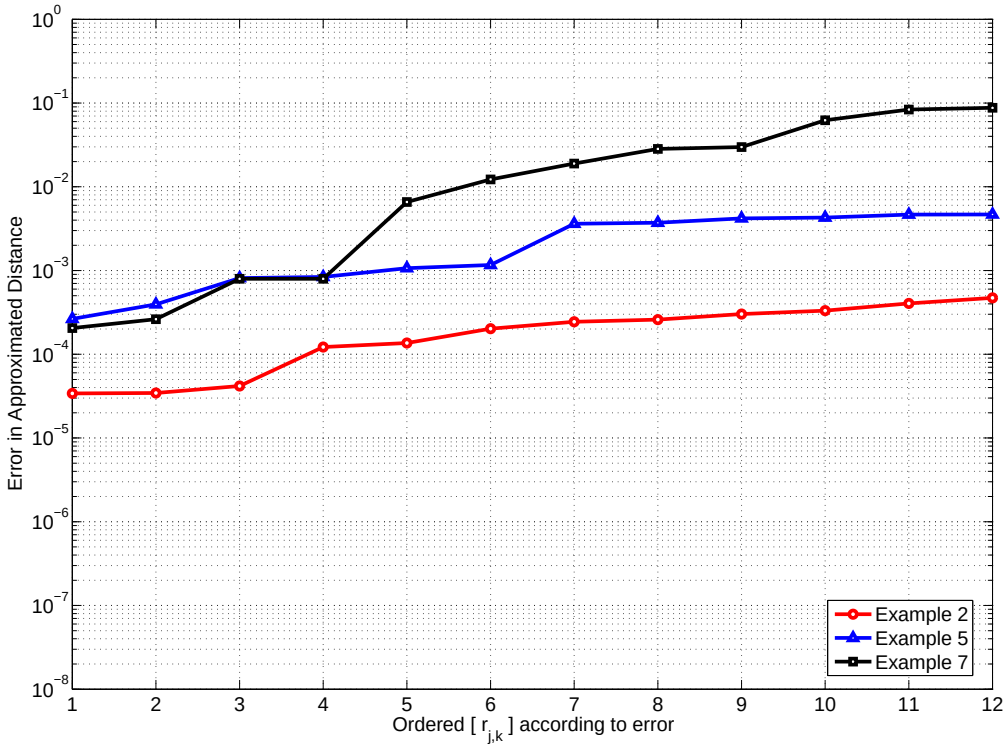

Figure 9. Error in approximate distance for each $r_{j,k}$ (sorted based on the errors), $1 \leq j \leq 3$ and $1 \leq k \leq N$ using $M = 3$ measurement points $\{b'_1, b'_2, b'_3\}$.